

Biomechanical Analysis of Lumbar Disc Degeneration Before and After Spinal Fusion

Maria Inês Vieira Godinho
inesgodinho@tecnico.ulisboa.pt

Instituto Superior Técnico, Lisboa, Portugal
December 2020

Abstract

Advancing age and degeneration frequently lead to low back pain (LBP), which is the most prevalent musculoskeletal disorder worldwide. Changes in the ligamentous structures and intervertebral discs (IVD) are typically amongst the sources of instability. Spinal fusion techniques are therefore at the core of treatment options to remove the affected IVD and relieve LBP. The aim of this work was three-fold: (i) to understand how ligament degeneration links with LBP by determining the role of each ligament per movement, (ii) to evaluate the impact of disc height reduction in degenerative changes, and (iii) to assess the more advantageous type of posterior fixation in interbody fusion to support clinical practice, particularly regarding adjacent disc degeneration (ADD). For that, two L3-L5 finite element models with different IVD heights were used. Different degrees of ligament and IVD degeneration were tested, and the Oblique Lumbar Interbody Fusion (OLIF) procedure was simulated with different fixation constructs. Facet capsular ligament and anterior longitudinal ligament were identified as the most influential ligaments for spinal stability, being this influence enhanced with degeneration and IVD height reduction. After spinal fusion, these ligaments became obsolete. The OLIF procedure contributed more to ADD than degeneration of the pre-instrumented level, with bilateral fixation being the best option to achieve stability and lessen ADD risk. Between models with unilateral constructs, right unilateral fixation was the most suited to reduce IVD stress. Clinical practice will benefit from the outcomes of this study and from its future extension to a wider patient database.

Keywords: Lumbar Spine, Ligaments, Degeneration, Interbody Fusion, Biomechanics, Finite Element Modelling

1. Background

With advancing age and degeneration, several changes are induced in the spine. These can possibly lead to different pathological conditions and ultimately culminate in low back pain (LBP), which is the most prevalent musculoskeletal disorder and a major source of disability worldwide [1]. Changes in the ligamentous structures or the intervertebral discs (IVDs) are common causes of LBP, and they can be interconnected, thus leading to further damage [2]. Therefore, it is important to understand the processes of degeneration of ligaments and IVDs, as well as their contribution to spine kinematics.

For the disorders originating from degeneration, several treatment options are available, from medication and physical therapy to surgical procedures in cases of severe pathology [3]. Spinal fusion techniques are typical surgical procedures with the intent of eliminating LBP. The focus of the present work is interbody fusion, in which the degenerated IVD is removed and a cage is inserted in its place, with additional bone graft to promote fusion. There are several approaches for cage introduction, but in the current work the Oblique Lumbar Interbody Fusion (OLIF) procedure was simulated. In spinal fusion, posterior fixation may or may not be supplemented

and its use has been widely researched over the years. However, there is still some debate about whether bilateral fixation systems are required to stabilise the spinal segment or if unilateral constructs are enough to maintain the cage in place and promote bone fusion [4]. Some studies have found unilateral instrumentation to be as effective as bilateral systems, with clinical studies indicating similar rates of fusion and implant failure for both constructs [4]–[6]. Other biomechanical and finite element (FE) studies have shown bilateral fixation systems to provide greater spinal and implant stability [7]–[9].

To evaluate the biomechanics of the spine and devise solutions for this type of questions, the FE method is a very useful tool to ensure reproducibility of results without destroying the test samples.

Although there have been several studies evaluating the mechanical properties of healthy spinal ligaments and IVD degeneration [10]–[14], the process of ligament degeneration and its effects on spinal kinematics are still unclear. To the author's knowledge, there are no FE studies focused on ligament changes with degeneration. Moreover, regarding ligament removal and morphological degeneration (namely disc height

reduction), it is also important to further understand their impact on the stability of a degenerated spine, as well as the changes induced in adjacent levels. From the degenerated spine, treatment decisions can benefit from in-depth FE simulations of different scenarios to support clinical practice with enhanced data. With this in mind, the aim of this work was three-fold:

- i. to explore the role of each ligament per movement and determine the effects of ligament degeneration on spine kinematics
- ii. to evaluate the impact of disc height reduction in degenerative changes
- iii. to assess the more advantageous type of posterior fixation in interbody fusion to support clinical practice, particularly regarding adjacent disc degeneration (ADD).

2. Materials and Methods

For the current work, two different L3-L5 FE models were used. The first, developed and validated in a previous work [3], was used to evaluate the role of ligaments and the process of ligament degeneration. The second, devised in the current work, was constructed with the purpose of assessing the influence of disc height reduction in degenerative changes and simulate spinal fusion.

2.1. Ligament Modelling

2.1.1. FE model

The model used in the first part of this work was developed in a previous study [3], based on computer tomography (CT) scans from a healthy 40-year-old woman (Figure 1). It included three vertebrae (L3 to L5), two IVDs, divided into annulus fibrosus (AF) and nucleus pulposus (NP), and the seven major ligaments of the lumbar spine modelled as linear elastic tension-only spring elements: anterior longitudinal ligament (ALL), posterior longitudinal ligament (PLL), facet capsular ligament (FCL), ligamentum flavum (LF), interspinous ligament (ISL), intertransverse ligament (ITL) and supraspinous ligament (SSL).

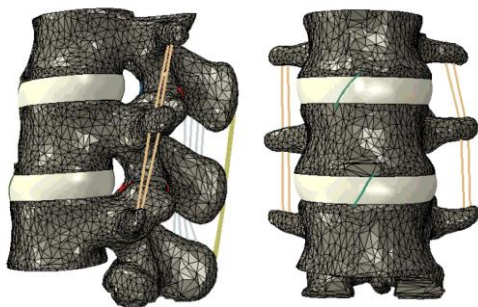


Figure 1: Sagittal (left) and frontal (right) views of the FE model used in the first part of this work.

Material properties of the model components were taken from the literature [12], [13], [15], [16] and are presented in Table 1.

In all cases, a pre-load of 100 N [10] and a moment of 7.5 Nm were applied, with boundary conditions completely restraining the movement of L5. The main outcome of the simulations was range of motion (ROM), namely the relative ROM changes.

Table 1: Material properties assigned to each model component.

Material	Formulation	Parameters
Cortical Bone	Linear Elastic	$E = 1200 \text{ MPa}$ $\nu = 0.3$
Trabecular Bone	Linear Elastic	$E = 200 \text{ MPa}$ $\nu = 0.315$
Nucleus Pulposus	Hyperelastic Isotropic (Mooney-Rivlin)	$C_{10} = 0.120 \text{ MPa}$ $C_{01} = 0.030 \text{ MPa}$ $D_1 = 0.667 \text{ MPa}^{-1}$
Annulus Fibrosus	Hyperelastic Anisotropic (Holzapfel)	$C_{10} = 0.315 \text{ MPa}$ $D_1 = 0.254 \text{ MPa}^{-1}$ $k_1 = 12 \text{ MPa}$ $k_2 = 300$ $\kappa = 0.1$
ALL	Linear Elastic	$E = 20.0 \text{ MPa}$ $A = 75.9 \text{ mm}^2$
PLL	Linear Elastic	$E = 10.0 \text{ MPa}$ $A = 1.6 \text{ mm}^2$
FCL	Linear Elastic	$E = 7.5 \text{ MPa}$ $A = 19.0 \text{ mm}^2$
LF	Linear Elastic	$E = 13.0 \text{ MPa}$ $A = 39.0 \text{ mm}^2$
ITL	Linear Elastic	$E = 12.0 \text{ MPa}$ $A = 1.8 \text{ mm}^2$
ISL	Linear Elastic	$E = 9.8 \text{ MPa}$ $A = 12.0 \text{ mm}^2$
SSL	Linear Elastic	$E = 8.8 \text{ MPa}$ $A = 6.0 \text{ mm}^2$

2.1.2. Ligament Removal

To evaluate the impact of each ligament in the movement, a four-phase ligament removal process was established, adapted from the work of Ellingson et al. [12]: (i) removal of superficial ligaments (ISL, ITL, SSL, LF), (ii) FCL removal, (iii) PLL removal, and (iv) ALL removal with different degrees of disc degeneration. The removal process was conducted twice for each model: (1) removing ligaments only in L4-L5, given that this is usually the segment most affected by degeneration [17], and (2) removing all ligaments in both L3-L4 and L4-L5 levels. These will be referred to as cases 1 and 2, respectively.

Different cases of IVD degeneration were considered by assigning different material properties to each IVD. Geometrical parameters, such as disc height, were not altered. Table 2 shows the material properties assigned to the IVD components based on the evolution of degeneration presented in the literature. Three

degenerated cases were created by combining two different degeneration IVD stages (mild and moderate) with the healthy state: Healthy-Mild (H-Mild), Mild-Mild, and Mild-Moderate (Mild-Mod).

Table 2: Material properties assigned to each IVD component in different degeneration stages.

Deg. Stage	Annulus Fibrosus	Nucleus Pulposus
Healthy	$C_{10} = 0.315 \text{ MPa}$ $D_1 = 0.254 \text{ MPa}^{-1}$ $k_1 = 12 \text{ MPa}$ $k_2 = 300$	$C_{10} = 0.120 \text{ MPa}$ $C_{01} = 0.030 \text{ MPa}$ $D_1 = 0.667 \text{ MPa}^{-1}$
Mild	$C_{10} = 0.500 \text{ MPa}$ $D_1 = 0.320 \text{ MPa}^{-1}$ $k_1 = 1.74 \text{ MPa}$ $k_2 = 43.5$	$C_{10} = 0.168 \text{ MPa}$ $C_{01} = 0.042 \text{ MPa}$ $D_1 = 0.476 \text{ MPa}^{-1}$
Moderate	$C_{10} = 1.130 \text{ MPa}$ $D_1 = 0.140 \text{ MPa}^{-1}$ $k_1 = 0.435 \text{ MPa}$ $k_2 = 8.7$	$C_{10} = 0.221 \text{ MPa}$ $C_{01} = 0.055 \text{ MPa}$ $D_1 = 0.723 \text{ MPa}^{-1}$

Deg. Stage – Degeneration Stage

2.1.3. Ligament Degeneration

Regarding ligament degeneration and its impact on spine biomechanics, this process can be evaluated by changing the mechanical properties of ligaments, namely their stiffness. First, it is important to consider that the degeneration process may have different origins, and also occur in different stages. In this particular case, the focus is on age-related ligament degeneration and, based on the literature [18]–[21], the following two-stage ligament degeneration process was considered, assuming that disc degeneration occurs first [22]: (i) ligament relaxation (i.e. stiffness decrease) due to reduced mobility of the discs, and (ii) increase in ligament stiffness due to collagen cross-linking.

The simulations in this work considered that ligament stiffness is first decreased, and then increased, to study the effects of degeneration in the first and second stages of this process, respectively. Reductions in stiffness of 25%, 50% and 75% were tested. For simplicity purposes, ligament degeneration was mainly focused on the ligaments intervening on spine movement; otherwise, degeneration would have no significant impact. Therefore, only ALL and FCL were degenerated, given that, from the results obtained in this work, these are the ligaments that showed the most significant impact on movement. Nonetheless, this may be a limitation since ligament degeneration is unlikely to be an isolated event. Other simulations were hence tested in which all ligaments were degenerated in the same proportion, since there is no information about which ligaments degenerate together and in which

way. However, this remains an approximation as it is also not very likely for all ligaments to degenerate exactly at the same time and in the same proportion.

2.2. Morphological Degeneration and Spinal Fusion

2.2.1. Intact model

The model constructed in the second part of this work was based on CT scans from a 78-year-old woman, available on the xVertSeg Database from the Laboratory of Imaging Technologies (University of Ljubljana, Faculty of Electrical Engineering, Slovenia). This particular set of images was chosen due to the reduced IVD height presented by this subject. Geometry of L3-L5 vertebrae was obtained through image segmentation using ITK-SNAP® [23], and the IVDs were posteriorly introduced in SolidWorks® (Dassault Systèmes SolidWorks Corp., USA), having as reference the space between adjacent vertebrae in the CT images. These were also divided into AF and NP with cross-sectional proportions of 70% and 30%, respectively [24]. The model was then imported into FE solver ABAQUS® (Dassault Systèmes Simulia Corp., USA), where the seven major ligaments of the lumbar spine were added and annular fibres were oriented at 35 or 145 degrees in consecutive layers relative to the transverse plane. The model was considered rigidly bonded, and the same material properties as in section 2.1.1 (Table 1) were assigned to each model component. Facet joints were modelled with a gap of 1 mm and the contacts between them were defined as surface-to-surface soft contact with exponential-pressure-overclosure option (fit parameters: pressure of 50 N/mm², clearance of 1 mm). The same boundary conditions of the previous model were applied: inferior endplate of L5 was constrained from moving in any of the three principal directions, and moments of 7.5 Nm were applied in a reference point defined on the top surface of L3, to simulate extension/flexion, axial rotation (AR), and lateral bending (LB) movements.

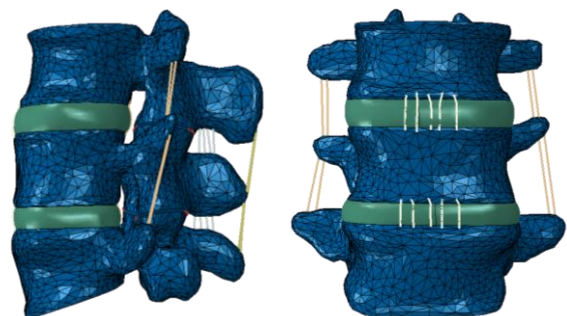


Figure 2: Sagittal (left) and frontal (right) views of the intact L3-L5 FE model.

The final model was composed of three vertebrae and two IVDs, generating 230 051 C3D10 mesh elements, together with 172 T3D2 elements representing the ligaments (Figure 2). The model was validated against the work presented by Heuer et al. [13], following the same ROM trends, but with lower absolute values due to increased degeneration and IVD height reduction.

2.2.2. Degenerated models

To include the degenerative changes apart from the intrinsic IVD height reduction, the intact model presented in the previous subsection was modified. In a first analysis, only IVDs were degenerated, following the same principles used in the first model, described in section 2.1.2. Material properties of AF and NP were altered, creating four models with different combinations of IVD degeneration (apart from the healthy one): H-Mild, Mild-Mild, H-Mod, and Mild-Mod. For ligament degeneration, the same methodology described in section 2.1.3 was applied.

2.2.3. Instrumented models

From the intact model, four instrumented models were constructed to simulate the OLIF procedure and evaluate the influence of posterior fixation: stand-alone cage model (SA), model with left unilateral posterior fixation (LUPF), model with right unilateral posterior fixation (RUPF), and model with bilateral posterior fixation (BPF). For that, the L4-L5 IVD was removed in SolidWorks® – as this was the most degenerated IVD – and a CLYDESDALE® cage system (CLYDESDALE Spinal System; Medtronic Sofamor Danek USA, Inc., Memphis, Tennessee, USA) was introduced in its place, virtually mimicking the OLIF surgical procedure [25]. For the models with posterior fixation, additional screws were added through the right and/or left pedicles with a rod connecting them, simulating unilateral or bilateral fixations.

The models of the cage, rod, and screws were adapted from previous work [26]. The height, width, and length of the OLIF cage were 8 mm, 22 mm, and 50 mm, respectively. The length and diameter of the pedicle screws were 55 mm and 5.5 mm, respectively. The diameter of the rod was the same as the screws [25].

The instrumented models were then imported to ABAQUS® and the same process as in the intact model was followed, with the exception that this time two different analyses were required to evaluate the biomechanical impact of the cage: short-term and long-term analyses. In the short term, bone-screw interactions were modelled as being fully bonded with a *tie* constraint, while cage-bone interactions were defined as surface-to-surface contact with a friction coefficient of 0.8. In the long term, all model components were assumed to be rigidly bonded using the merge

tool, mimicking the bone ingrowth and vertebral fusion that occurs. Material properties were also assigned to each instrumentation component, being the cage composed of PEEK and the rod and screws of a titanium alloy (Table 3).

Table 3: Material properties assigned to instrumentation components.

Material	Formulation	Parameters [26]
PEEK	Linear Elastic	$E = 3600 \text{ MPa}$ $\nu = 0.38$
Titanium	Linear Elastic	$E = 105\,000 \text{ MPa}$ $\nu = 0.34$

3. Results and Discussion

The results of this work are reported in two levels of analysis. First, ligament modelling outcomes are presented, including the influence of ligament removal and degeneration on spine kinematics. Second, the biomechanical behaviour of the lumbar spine with morphological IVD degeneration and subsequent spinal fusion is presented.

3.1. Ligament modelling

3.1.1. Ligament removal

Table 4 presents the outcomes for a model with healthy IVDs and removed ligaments. In terms of AR, all ligaments presented almost zero influence in the movement, whereas in flexion, FCL was the ligament that influenced this movement the most, with an increase in ROM of 19.42% in case 1 and 10.91% in case 2. This is in agreement with the literature [12], [27], [28].

Regarding extension, the superficial ligaments and FCL had no influence in this movement. The ligament that presented the highest level of influence was ALL (ROM change of 14.12% and 13.78% in cases 1 and 2, respectively). This is in line with Heuer et al. [13] that reported a lack of influence of PLL in extension, and other studies that highlight the significant mechanical role of ALL in extension [2], [14], [24].

In LB, all ligaments presented a low influence in movement restriction. The only exception was ALL, with an increase in ROM of 9.72% and 9.23% in relation to the previous stage, in cases 1 and 2, respectively.

When comparing the outcomes between cases 1 and 2, ROM changes in case 2 were higher than analogous changes in case 1, which is justified by the less restricted movement occurring when ligaments are removed from all levels (case 2). However, there were a few exceptions in which ROM changes in L4-L5 decreased from case 1 to case 2: FCL and superficial ligaments in flexion, and FCL and ALL in LB. This was due to the boundary conditions applied in L5, which limited

the motion of L4-L5. Therefore, when the two levels were unrestricted, L3-L4 functional spinal unit (FSU) could move freely, and accumulated the movement that L4-L5 could not perform. This suggests a compensation mechanism between both segments and justifies the larger ROM changes in L3-L4 relatively to analogous changes in L4-L5. In this way, it is justified, for example in the case of FCL in flexion, the decrease of a ROM per cent change (ROM p.c.) of 19.42% in case 1 to 10.91% in case 2, considering that there is a compensation in L3-L4 with an increase from - 1.84% to 36.26%.

Table 4: Segmental ROM p.c. (%) with ligament removal as a function of movement.

			Sup.L	FCL	PLL	ALL
AR	Case 1	L3-L4	0.00	0.63	0.05	-0.01
		L4-L5	0.00	0.45	0.00	0.00
	Case 2	L3-L4	0.00	2.34	0.03	0.00
		L4-L5	0.00	0.54	0.02	0.00
F	Case 1	L3-L4	0.11	-1.84	0.00	0.00
		L4-L5	4.86	19.42	0.00	0.00
	Case 2	L3-L4	12.85	36.26	0.58	0.00
		L4-L5	2.36	10.91	-0.14	0.00
E	Case 1	L3-L4	0.00	0.00	0.00	-0.53
		L4-L5	0.00	0.00	0.00	14.12
	Case 2	L3-L4	0.00	0.00	0.00	6.58
		L4-L5	0.00	0.00	0.00	13.78
LB	Case 1	L3-L4	0.00	0.10	0.00	-0.30
		L4-L5	0.00	2.67	0.00	9.72
	Case 2	L3-L4	0.16	6.44	0.01	7.42
		L4-L5	-0.02	1.70	0.00	9.23

Sup.L – superficial ligaments (ISL, ITL, SSL, and LF)

Considering IVD degeneration, the outcomes were slightly different relatively to the healthy model. In AR, FCL presented in this case a significant impact in the movement, with a ROM change of around 10% in the degenerated models compared with less than 1% in the healthy model. In extension, ALL remained the most active ligament. However, its influence was decreased with progressive degeneration, from 14.12% ROM change in the healthy model to 8.13% in the most degenerated case. Regarding LB, similarly to extension, ALL remained the ligament with most impact, but in the degenerated models there was a decrease in influence (ROM p.c. decreased from 9.72% to 2.40%), given that ROM was already increased due to IVD degeneration and, consequently, the increase due to ligament removal could not be as pronounced to prevent excessive motion. Therefore, in cases of mild degeneration, in which the increase in ROM due to fibre laxity was higher, the increase due to ALL removal was lower. In cases with more advanced degeneration, since IVD stiffness led to a decrease in ROM, removing ALL increased ROM

change. Finally, when it comes to flexion, FCL remained the ligament with greatest influence. Comparing the multiple degenerated models, it was also possible to conclude that IVD degeneration and motion restriction may be highly influenced by adjacent levels.

3.1.2. Ligament degeneration

Besides ligament removal, ligament degeneration must be considered when evaluating spinal stability. In the first stage, with stiffness reduction, there was a slight increase in ROM for flexion and AR when FCL was degenerated (ROM p.c. of 3.58% and 2.38%, respectively), and for extension in the case of ALL (ROM p.c. of 0.56%). With overall degeneration, ROM variations were very similar, confirming that ALL and FCL were ruling the movement. In the second stage, FCL and ALL remained the most active ligaments in flexion and AR, and extension, respectively, but this time inducing negative ROM changes since ligament stiffness increased and the motion was hampered. ROM changes were more pronounced as the percentage of ligament degeneration was increased.

When comparing the outcomes between models with different IVD degeneration, it was verified that ROM relative changes with mild ligament degeneration were slightly higher in the model with the most advanced stage of IVD degeneration. This indicates that ligament degeneration is influenced by IVD degeneration.

3.2. Morphological Degeneration and Spinal Fusion

The main outcomes of the second set of simulations in this work were the ROM and stress values in the IVDs to evaluate the influence of morphological changes and the stability of the spine before and after spinal fusion. ROM values were determined in L4-L5 and L3-L4 levels to evaluate spinal stability and the effects on the adjacent level (Figure 3).

3.2.1. IVD degeneration

Assuming an increasing degenerative state from H-H to Mild-Mod model, global ROM values increased in the first stages of degeneration, until the state with both discs mildly degenerated, and then started decreasing as degeneration became more pronounced. This is in agreement with the process of disc degeneration and previously obtained results, including the results of the model without morphological degeneration (WOMD) [3], [11]. The greatest increase in ROM, of around 40%, occurred for AR from the healthy to the H-Mild model. When compared with the previous model in Figure 1, WOMD, absolute ROM values were generally lower in the model with morphological degeneration (WMD) for all loading

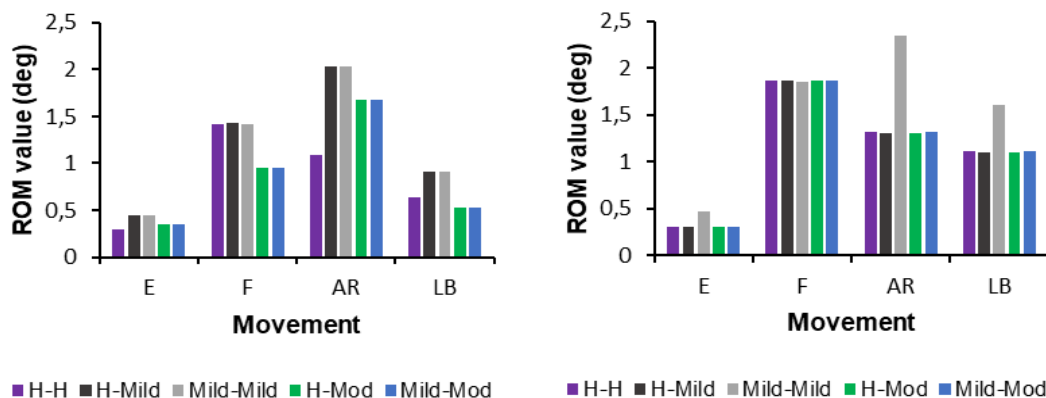


Figure 3: ROM evolution of the L3-L5 FE model with progressive IVD degeneration for different movements at L4-L5 (left) and L3-L4 levels (right).

directions, since the decreased IVD height is associated with a loss of hydration by the NP, therefore increasing IVD stiffness and restricting motion.

The abovementioned observations apply to all movements, except flexion. The main difference of this movement in relation to the others occurred for the early stages of degeneration, in which ROM remained the same as in the healthy model and did not increase. This situation could possibly be a result of the model's morphological changes: since there was a decrease in disc height, there was a lower ROM allowed before bone was reached. With advancing degeneration, ROM values decreased as before.

In terms of supported loads, the trends were the same throughout all models given that, according to the movement that is performed, the same IVD regions will be under stress. In the case of extension/flexion, there was more load supported by the anterior/posterior regions, respectively, which are high tension regions. For LB, the right IVD region was the most active under tension. Regarding AR, all IVD regions were under similar tension, except for the posterior region, which was subjected to lower loads. From Table 5, it is possible to conclude that the loads supported by L3-L4 IVD were in general higher than the ones supported by L4-L5 IVD. This was possibly due to the height reduction in L4-L5 IVD, but mainly to the closest proximity between L3-L4 IVD and the point of application of the load. When the disc had a mild degeneration, there was a decrease in the supported load for any movement, for both IVDs. From the healthy to H-Mild model, there was a reduction in L4-L5 ROM of around 15%, 48%, 63%, and 45% for LB, E, F, and AR, respectively. When the degeneration increased, the load increased due to disc stiffening, except for AR. However, this was only visible for L4-L5 IVD since L3-L4 IVD was mildly degenerated at most. From Mild-Mild to H-Mod model, L4-L5 ROM

increased by approximately 23%, 46%, 75% for LB, E, and F, respectively, and decreased 22% for AR.

3.2.2. Ligament degeneration

When considering the first ligament degeneration stage (Mild-Mild), the same trends as in the model WOMD were verified. Nonetheless, the increase in ROM due to stiffness reduction was enhanced: in flexion and AR, when FCL was degenerated, ROM increased 11.10% and 5.71%, respectively, compared with 3.92% and 2.40% in the model WOMD; similarly, in extension, with ALL degeneration, ROM increased 1.12%, compared with 0.66% in the model WOMD.

Regarding the second degeneration stage (Mild-Moderate), FCL and ALL remained the ligaments with greatest impact in flexion and AR, and extension, respectively. However, ROM changes at the L4-L5 level were more negative relative to the model WOMD, being the motion more restricted with the same increase in ligament stiffness (ROM changes of - 6.99%, - 3.31%, and - 0.89% compared with - 3.71%, - 1.49%, and - 0.70%, for flexion, AR, and extension, respectively). With progressive degeneration, i.e. with increasing percentages of variation in ligament stiffness (namely, 50% and 75%), the abovementioned outcomes were also verified, but with more pronounced ROM changes.

Comparing the results from the simulations in which ALL and FCL were degenerated as a set with the ones of overall degeneration, ROM variations were very similar for extension, as in the model WOMD. In the case of AR and flexion, differences between ROM changes with FCL vs. overall degeneration were higher. This shows that, besides FCL that was the most active ligament, the remaining ligaments also had small contributions to the movement that became significant when added. In the case of flexion,

Table 5: Stress values (in MPa) in the IVDs as a function of movement and model degeneration, for each L3-L4 and L4-L5 levels.

		H-H	H-Mild	Mild-Mild	H-Mod	Mild-Mod
L3-L4	LB	0.4026	0.4019	0.3175	0.4033	0.3179
	E	0.2350	0.2324	0.1097	0.2340	0.1102
	F	0.3719	0.3705	0.1387	0.3734	0.1397
	AR	0.3320	0.3319	0.1883	0.3318	0.1882
L4-L5	LB	0.3244	0.2747	0.2732	0.3368	0.3348
	E	0.2631	0.1361	0.1350	0.1970	0.1947
	F	0.3419	0.1259	0.1254	0.2197	0.2187
	AR	0.3705	0.2028	0.2028	0.1583	0.1583

in particular, are highlighted the contributions of ISL and LF since their impact in ROM increase was higher than the one of the remaining ligaments (although not as significant as the one of FCL). For example, in the first stage of degeneration with a reduction in ligament stiffness of 50%, ISL and LF led to an increase in ROM of around 5% each, whereas FCL degeneration increased ROM by 24.13%. In general, the results for ligament degeneration followed the same trends verified for the FE model WOMD. However, ROM variations were more pronounced in the case WMD, leading to believe that an increased IVD degeneration, including IVD height reduction, results in an increased ligament degeneration as well. This is a good indicator that ligament degeneration follows IVD degeneration.

3.2.3. Instrumented models

Regarding the OLIF procedure, the introduction of instrumentation led to a marked ROM decrease from the intact model for all loading directions in the long-term (Figure 4).

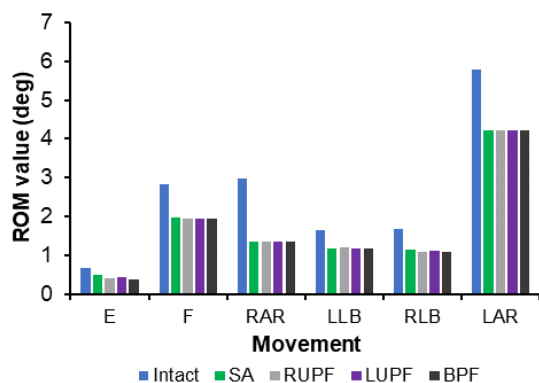


Figure 4: Global ROM values of the different instrumented models as a function of movement in long-term analysis (RAR – right AR; LLB – left LB; RLB – right LB; LAR – left AR).

The greatest decrease with cage introduction occurred for AR, with a ROM value around 55% lower than in the intact model, followed by LB and flexion (ROM reduction of around 30%). However, given that the long-

term goal with the introduction of instrumentation is spinal fusion, a decline in ROM values is expectable, especially in the intervened L4-L5 level (the movement of the bottom FSU was practically zero in all directions). Comparing the SA model with the models with posterior fixation, ROM decreased slightly further in the models with unilateral fixation and even more in the BPF model, particularly for extension. Extension was the movement in which differences in fixation had the strongest impact.

In short-term, when osseointegration is being established, ROM trends were slightly different compared with the case of complete spinal fusion. Considering global ROM values, there was a significant ROM increase from the intact to the SA model for all loading directions. The greatest increase occurred in extension, followed by right AR (RAR). For these movements, ROM was around four and three times higher in SA than in the intact model, respectively. With the introduction of posterior fixation, it was verified a decrease in mobility, especially with the introduction of a bilateral fixation system, similar to what occurred in long-term.

Considering a stress analysis in the adjacent IVD (Table 6), there was an increase in supported load during LB and flexion (18.5% and 10.2%, respectively), and a decrease during extension and AR (8.52% and 7.34%, respectively) from the intact to the SA model. With the introduction of posterior fixation, a reduction in IVD load should be expected due to load-sharing. However, with a focus on unilateral fixation outcomes, this situation only occurred for flexion and right LB (RLB) in RUPF, and for LB in LUPF. The load increase in the remaining loading directions might therefore contribute to accelerate adjacent degeneration. With the introduction of bilateral fixation, it was possible to remove load from the IVD, leading to a reduction in stress values from SA to BPF models for all movements, except extension. The greatest decrease occurred for flexion, with a stress variation of around 24%. Between both models with

Table 6: Stress values (in MPa) supported by L3-L4 IVD in the different instrumented models as a function of movement in long-term simulations. Between brackets are the p.c. in relation to the SA model (or intact model in the case of SA).

	Intact	SA	RUPF	LUPF	BPF
E	0.2340	0.2141 (-8.52%)	0.2428 (13.4%)	0.2639 (23.3%)	0.2283 (6.64%)
F	0.3734	0.4116 (10.2%)	0.2670 (-35.1%)	0.4821 (17.1%)	0.3138 (-23.8%)
RAR	0.3318	0.3074 (-7.34)	0.3083 (0.28%)	0.3237 (5.30%)	0.2981 (-3.02%)
LLB	0.4033	0.4780 (18.5%)	0.5284 (10.5%)	0.4550 (-4.80%)	0.3825 (-20.0%)
RLB		0.4232	0.4177 (-1.30%)	0.4133 (-2.33%)	0.4257 (0.60%)
LAR		0.0979	0.0988 (0.94%)	0.1115 (13.9%)	0.0783 (-20.1%)

Table 7: Instrumentation stress values (in MPa) in the different instrumented models as a function of movement in long-term simulations. Between brackets are the p.c. in relation to the SA model.

	Cage				Posterior Fixation		
	SA	RUPF	LUPF	BPF	RUPF	LUPF	BPF
E	12.67	6.520 (-48.5%)	5.792 (-54.3%)	3.992 (-68.5%)	42.21	40.45	32.76
F	6.627	5.030 (-24.1%)	5.375 (-18.9%)	4.138 (-37.6%)	26.97	26.51	20.18
RAR	4.061	3.457 (-14.9%)	3.604 (-11.3%)	3.039 (-25.2%)	21.56	16.91	20.64
LLB	5.681	5.614 (-1.18%)	4.473 (-21.3%)	4.248 (-25.2%)	10.60	14.24	16.31
RLB	5.693	4.582 (-19.5%)	5.672 (-0.37%)	4.192 (-26.4%)	14.32	9.41	16.43
LAR	4.313	3.093 (-28.3%)	3.945 (-8.53%)	2.934 (-32.0%)	25.28	16.48	25.97

unilateral constructs, LUPF presented higher stresses acting on the IVD compared with RUPF, except for LB. This may be a result of the asymmetry of cage placement. Since the cage is introduced from the left side of the body, it is therefore subjected to higher loads on this side, relieving the load acting on the left portion of the adjacent IVD. In fact, in the SA model, the right portion of the IVD withstood higher loads for all loading directions. Posterior fixation is thus more useful on the right side of the body, explaining the lower stress values of the IVD in the RUPF model.

The stress acting on the cage was always higher in the cage-only model, comparing the four models with and without posterior fixation, which may lead to an increased risk of cage subsidence and implant migration (Table 7). The greatest load support occurred for movements in the sagittal plane: extension (12.67 MPa), followed by flexion (6.627 MPa). With the introduction of posterior fixation, cage stress was reduced, especially with bilateral fixation, due to an increased load-sharing between constructs. The greatest load decrease occurred in the BPF model for all loading directions, being more significant in extension (decrease of 68.5%), followed by flexion (decrease of 37.6%).

The posterior fixation stress was the highest in extension, followed by flexion. However, the supported loads were in general higher than in the cage to avoid cage subsidence. As before, the introduction of bilateral fixation led to the highest stress reduction, but, in this case, it was only verified for extension and flexion. For the remaining movements, stress values were lower in the model with left unilateral construct

given that, due to cage asymmetry, posterior fixation on the left side was not so critical. Since the BPF model includes right unilateral fixation in addition to the left construct, and that fixation on the right side is required for support (supporting higher loads), the loads exerted on the instrumentation increased. Comparing RUPF and LUPF models, the stress acting on the left unilateral construct was lower than the one on the right for the same reasons abovementioned, namely cage asymmetry. Moreover, the load supported by the adjacent IVD was lower in the RUPF model, thus requiring the instrumentation to support higher loads. This was true for every movement except left LB (LLB). In this case, loads were higher in the LUPF model since the instrumentation will be under increased stress if the movement occurs towards the side of fixation.

The stress supported by the instrumentation was higher in short-term simulations. In any case, there was no risk of failure or screw loosening since all values were significantly below the ultimate tensile strength of titanium alloys (500 – 1000 MPa [29]) or PEEK (100 MPa [30]), in the case of posterior instrumentation and the cage, respectively.

Regarding the role of ligaments, these structures presented a restrictive behaviour in the short-term. They maintained the cage in place and avoided its migration, contributing to spinal fusion. However, in the long-term, since everything is completely osseointegrated, ligaments became obsolete.

Finally, if degeneration was considered on the adjacent IVD, the spine became less stable for all loading directions, except flexion and left

AR (LAR), and stress values acting on the disc were smaller than the ones acting on a healthy IVD.

3.2.4. Adjacent Disc Degeneration

ADD is a serious spinal condition since it affects the long-term success of interbody fusion surgery, possibly resulting in the recurrence of LBP and radiculopathy. Although the definite mechanisms of this condition are not yet fully clarified, previous studies have identified increases in ROM and intradiscal pressure (IDP) as the most probable causes [31]. In the case of lumbar spinal fusion, it is important to understand whether ADD is promoted by implant insertion and segmental fusion, or if there were already signs of ADD before surgery due to IVD degeneration.

In general, the stresses acting on the IVD and ROM values of the top FSU were higher in instrumented models than in degenerated intact models, even if the most advanced stage of degeneration was considered. Therefore, the OLIF procedure presented a higher contribution to ADD than L4-L5 IVD degeneration. The introduction of bilateral fixation may help lessen this contribution since, compared with the remaining instrumented models, the mobility and stresses supported by L3-L4 IVD were decreased. These outcomes are aligned with the literature. Although some papers suggest that ADD results of the natural progression of degeneration and is not affected by lumbar fusion, the majority show that lumbar fusion plays, in fact, a key role in the development of ADD, and that adjacent ROM and IDP increase in this situation [32], [33].

4. Conclusions

This work provides a new perspective on how degeneration and interbody fusion influence spinal stability, taking advantage of the insights that numerical simulations can provide for multiple situations.

FCL and ALL were determined to be the most influential ligaments in spinal stability, but the importance of the last was diluted with degeneration. The compensation mechanisms identified here, when ligaments are removed and/or degeneration progresses, along with adjacent level degeneration, are very relevant factors to be accounted for in clinical practice and potentially for fusion surgery recommendations. Moreover, the procedure for ligament degeneration established in this work and the finding that ligament degeneration follows IVD degeneration may be useful for future FE studies.

Current results showed that morphological

degeneration, namely IVD height reduction, together with changes in material properties lead to increasing ROM values in the early stages of degeneration, which then decrease as degeneration progresses and the IVD stiffens. This behaviour was also verified in the model WOMD, thus not being triggered by morphological degeneration in particular. Absolute ROM values were lower in the model WMD for all loading directions due to increased IVD stiffness.

Regarding instrumented models, for the OLIF procedure, it was shown that a stand-alone cage is not sufficient to provide solid stability and supplementary fixation must be introduced. From a biomechanical perspective, bilateral fixation is the best option since maximum stability and the lowest stresses are achieved with this fixation system. From a clinical perspective, unilateral fixation would be preferable due to its lowest morbidity. Models with left and right unilateral constructs presented similar ROM values, but the models with fixation on the left side resulted in higher stresses on the adjacent IVD. Therefore, right unilateral fixation may be a good option over left constructs to reduce IVD stress and degeneration, possibly because there is an additional support on the left side due to cage asymmetry. In all cases, ligaments help to keep the cage in place before spinal fusion occurs, but they lose function as osseointegration is achieved. This work also showed that instrument placement has a stronger influence on the degeneration of the adjacent level than the degeneration of the pre-instrumented L4-L5 IVD. As such, interbody fusion is a major contributing factor to ADD progression.

In future studies, some factors should be further explored since they may deepen the outcomes of the present work, namely (i) more complex modelling of IVD and ligaments, (ii) inclusion of screw thread and teeth on the cage surface, (iii) analysis of the order of ligament removal, (iv) extension of the models to the full lumbar spine and new patient data, with different levels/types of degeneration, and finally (v) introduction of osteoporosis in the models, as this is also an age-related condition that will most likely affect spinal behaviour and may be interconnected with IVD degeneration.

References

- [1] F. Balagué, B. Troussier, and J. J. Salminen, "Non-specific low back pain in children and adolescents: risk factors," *Eur. Spine J.*, vol. 8, no. 6, pp. 429–438, Dec. 1999.
- [2] J. Widmer, F. Cornaz, G. Scheibler, J. M. Spirig, J. G. Snedeker, and M. Farshad, "Biomechanical contribution of spinal structures to stability of the lumbar spine—novel biomechanical insights," *Spine J.*, May 2020.
- [3] V. Carvalho, "Finite element modelling of

- innovative interspinous process spacers for the lumbar spine Biomedical Engineering," Instituto Superior Técnico, 2019.
- [4] J. Godzik *et al.*, "Biomechanical Stability Afforded by Unilateral Versus Bilateral Pedicle Screw Fixation with and without Interbody Support Using Lateral Lumbar Interbody Fusion," *World Neurosurg.*, vol. 113, pp. e439–e445, May 2018.
- [5] J. Li, W. Wang, R. Zuo, and Y. Zhou, "Biomechanical Stability Before and After Graft Fusion with Unilateral and Bilateral Pedicle Screw Fixation: Finite Element Study," *World Neurosurg.*, vol. 123, pp. e228–e234, Mar. 2019.
- [6] W. Ding, Y. Chen, H. Liu, J. Wang, and Z. Zheng, "Comparison of unilateral versus bilateral pedicle screw fixation in lumbar interbody fusion: a meta-analysis," *Eur. Spine J.*, vol. 23, no. 2, pp. 395–403, Feb. 2014.
- [7] H. Guo *et al.*, "Stability Evaluation of Oblique Lumbar Interbody Fusion Constructs with Various Fixation Options: A Finite Element Analysis Based on Three-Dimensional Scanning Models," *World Neurosurg.*, vol. 138, pp. e530–e538, Jun. 2020.
- [8] S.-H. Chen, S.-C. Lin, W.-C. Tsai, C.-W. Wang, and S.-H. Chao, "Biomechanical comparison of unilateral and bilateral pedicle screws fixation for transforaminal lumbar interbody fusion after decompressive surgery -- a finite element analysis," *BMC Musculoskelet. Disord.*, vol. 13, no. 1, p. 72, Dec. 2012.
- [9] D. V. Ambati, E. K. Wright, R. A. Lehman, D. G. Kang, S. C. Wagner, and A. E. Dmitriev, "Bilateral pedicle screw fixation provides superior biomechanical stability in transforaminal lumbar interbody fusion: a finite element study," *Spine J.*, vol. 15, no. 8, pp. 1812–1822, Aug. 2015.
- [10] W. M. Park, K. Kim, and Y. H. Kim, "Effects of degenerated intervertebral discs on intersegmental rotations, intradiscal pressures, and facet joint forces of the whole lumbar spine," *Comput. Biol. Med.*, vol. 43, no. 9, pp. 1234–1240, Sep. 2013.
- [11] A. Rohlmann, T. Zander, H. Schmidt, H.-J. Wilke, and G. Bergmann, "Analysis of the influence of disc degeneration on the mechanical behaviour of a lumbar motion segment using the finite element method," *J. Biomech.*, vol. 39, no. 13, pp. 2484–2490, Jan. 2006.
- [12] A. M. Ellingson, M. N. Shaw, H. Giambini, and K.-N. An, "Comparative role of disc degeneration and ligament failure on functional mechanics of the lumbar spine," *Comput. Methods Biomech. Biomed. Engin.*, vol. 19, no. 9, pp. 1009–1018, Jul. 2016.
- [13] F. Heuer, H. Schmidt, Z. Klezl, L. Claes, and H.-J. Wilke, "Stepwise reduction of functional spinal structures increase range of motion and change lordosis angle," *J. Biomech.*, vol. 40, no. 2, pp. 271–280, Jan. 2007.
- [14] T. Zander, A. Rohlmann, and G. Bergmann, "Analysis of Simulated Single Ligament Transection on the Mechanical Behaviour of a Lumbar Functional Spinal Unit / Rechnerische Analyse des Einflusses der Bänder auf das mechanische Verhalten eines Bewegungssegments der Lendenwirbelsäule," *Biomed. Tech. Eng.*, vol. 49, no. 1–2, pp. 27–32, Jan. 2004.
- [15] B. Yu, C. Zhang, C. Qin, and H. Yuan, "FE modeling and analysis of L4-L5 lumbar segment under physiological loadings," *Technol. Heal. Care*, vol. 23, no. s2, pp. S383–S396, Jun. 2015.
- [16] R. Eberlein, G. A. Holzapfel, and M. Fröhlich, "Multi-segment FEA of the human lumbar spine including the heterogeneity of the annulus fibrosus," *Comput. Mech.*, vol. 34, no. 2, pp. 147–163, Jul. 2004.
- [17] S. Saleem, H. M. Aslam, M. A. K. Rehmani, A. Raees, A. A. Alvi, and J. Ashraf, "Lumbar Disc Degenerative Disease: Disc Degeneration Symptoms and Magnetic Resonance Image Findings," *Asian Spine J.*, vol. 7, no. 4, p. 322, 2013.
- [18] A. L. Nachemson and J. H. Evans, "Some mechanical properties of the third human lumbar interlaminar ligament (ligamentum flavum)," *J. Biomech.*, vol. 1, no. 3, pp. 211–220, Aug. 1968.
- [19] E. M. K. Barros, C. J. Rodrigues, N. R. Rodrigues, R. P. Oliveira, T. E. P. Barros, and A. J. Rodrigues, "Aging of the elastic and collagen fibers in the human cervical interspinous ligaments," *Spine J.*, vol. 2, no. 1, pp. 57–62, Jan. 2002.
- [20] M. M. Panjabi, V. K. Goel, and K. Takata, "Physiologic Strains in the Lumbar Spinal Ligaments," *Spine (Phila. Pa. 1976)*, vol. 7, no. 3, pp. 192–203, May 1982.
- [21] W. C. Whiting and R. F. Zernicke, *Biomechanics of Musculoskeletal Injury*. Human Kinetics Publishers, 2008.
- [22] A. Polikeit, L. P. Nolte, and S. J. Ferguson, "Simulated influence of osteoporosis and disc degeneration on the load transfer in a lumbar functional spinal unit," *J. Biomech.*, vol. 37, no. 7, pp. 1061–1069, Jul. 2004.
- [23] P. A. Yushkevich *et al.*, "User-guided 3D active contour segmentation of anatomical structures: Significantly improved efficiency and reliability," *Neuroimage*, vol. 31, no. 3, pp. 1116–1128, 2006.
- [24] S. Naserkhaki, N. Arjmand, A. Shirazi-Adl, F. Farahmand, and M. El-Rich, "Effects of eight different ligament property datasets on biomechanics of a lumbar L4-L5 finite element model," *J. Biomech.*, vol. 70, pp. 33–42, Mar. 2018.
- [25] Medtronic, "Oblique Lateral Interbody Fusion For L2 to L5 Surgical Technique."
- [26] J. Real, "Biomechanical Analysis of Fixation Devices for Lumbar Interbody Fusion," Instituto Superior Técnico, 2019.
- [27] M. A. Adams and P. Dolan, "Recent advances in lumbar spinal mechanics and their clinical significance," *Clin. Biomech.*, vol. 10, no. 1, pp. 3–19, Jan. 1995.
- [28] Y. Alapan, C. Demir, T. Kaner, R. Guclu, and S. İnceoğlu, "Instantaneous center of rotation behavior of the lumbar spine with ligament failure," *J. Neurosurg. Spine*, vol. 18, no. 6, pp. 617–626, Jun. 2013.
- [29] M. Niinomi, "Mechanical properties of biomedical titanium alloys," *Mater. Sci. Eng. A*, vol. 243, no. 1–2, pp. 231–236, Mar. 1998.
- [30] W. Wu, P. Geng, G. Li, D. Zhao, H. Zhang, and J. Zhao, "Influence of Layer Thickness and Raster Angle on the Mechanical Properties of 3D-Printed PEEK and a Comparative Mechanical Study between PEEK and ABS," *Materials (Basel)*, vol. 8, no. 9, pp. 5834–5846, Sep. 2015.
- [31] C. S. Lee *et al.*, "Risk factors for adjacent segment disease after lumbar fusion," *Eur. Spine J.*, vol. 18, no. 11, pp. 1637–1643, 2009.
- [32] S. Jiang and W. Li, "Biomechanical study of proximal adjacent segment degeneration after posterior lumbar interbody fusion and fixation: a finite element analysis," *J. Orthop. Surg. Res.*, vol. 14, no. 1, p. 135, Dec. 2019.
- [33] S. Tang and B. J. Rebolz, "Does anterior lumbar interbody fusion promote adjacent degeneration in degenerative disc disease? A finite element study," *J. Orthop. Sci.*, vol. 16, no. 2, pp. 221–228, Mar. 2011.